Korean J. Chem. Eng., **26**(1), 160-164 (2009)

Improvement of sensitivity in an interferometry by controlling pore size on the anodic aluminum oxide chip pore-widening technique

Hee Chul An, Jin Young An, and Byung-Woo Kim†

Department of Chemical Engineering, Sungkyunkwan University, Suwon 440-746, Korea
(*Received 25 August 2008 • accepted 26 October 2008*)

Abstract−The pore size of an anodic aluminum oxide (AAO) chip, as well as uniform pore distribution, is one of the key parameters that should be adjusted, by choosing the appropriate etching conditions, in order to enhance the sensitivity of an interferometer. In this study, the pore size of AAO chips was optimized and characterized in order to lower the detection limit of prostate specific antigen (PSA) in an interferometric immunoassay system. After pore widening for 30-50 min, the AAO pore size was increased approximately 2-fold larger than that before pore widening. A large increase in effective optical density (ΔEOT) was obtained from the AAO chip fabricated by pore-widening technique, which thereby lowered the PSA detection limit. The present study results are not sufficiently validated to enable the immediate application to immunoassay for prostate cancer (PCa) screening, but they do demonstrate that controlling pore size can positively affect the sensitivity and lower the detection limit.

Key words: Interferometry, Biosensor, Anodic Aluminum Oxide (AAO), Prostate Specific Antigen (PSA), Pore Widening

INTRODUCTION

Biosensor research has been driven by the desire to detect and classify biological interactions for medical applications, environmental monitoring, and basic mechanistic studies [1]. Optical biosensors have received significant attention for label-free biosensing, by employing sensitive methods such as surface plasmon resonance, ellipsometry, and interferometry, despite their lower sensitivity than fluorescent and luminescent detection [2]. Amongst these sensors, a Fabry-Perot interferometer, which uses the induced shift in the fringe pattern caused by the change in the refractive index of the medium upon molecular interactions of species in solution with immobilized ligands or receptors within the porous silicon (pSi), can be used as a sensitive method for biomolecular sensing [3]. This system has the advantages of high sensitivity, inexpensive system configuration, easy measurement, lack of any need for a waveguide, and high throughput with a multi-well biochip [4]. However, the non-uniform distribution of pore size and depth of a pSi chip for a Fabry-Perot interferometer leads to relatively low sensitivity with poor reproducibility [5].

Nanoporous anodic aluminum oxide (AAO) with self-organized, hexagonal arrays of uniform, parallel nanochannels has been intensively used as the starting material for fabricating various functional nanostructures, in application areas such as magnetic, electronic and optoelectronic devices, biosensors and photonics [6-12]. In comparison with pSi, AAO has more uniform pore size distribution and can easily extend the pore depth to more than 5 μm, thereby enhancing the sensitivity of an interferometer. In our previous study, where AAO was used as an alternative to the existing porous Si-based interferometer for the detection of DNA-damaging chemicals in the environment [4], the sensitivity was enhanced about 200-fold compared with results using pSi.

In this study, porous AAO (pAAO) was used as an alternative to pSi in an interferometric immunoassay system for the detection of prostate specific antigen (PSA). PSA has been identified as a valuable biomarker to screen prostate cancer (PCa) patients [13]. The major forms of PSA found in serum are complexes with two major extracellular serine protease inhibitors, α1-antichymotrypsin (PSA-ACT, MW 90 kDa) and α2-macroglobulin (PSA-AMG), and a free form (f-PSA, MW 34 kDa), among which the complex with PSA-ACT complex is predominant [14-17]. A total PSA level (T-PSA; sum of f-PSA and PSA-ACT complex) of 10 ng/ml or lower is a highly probable indication for PCa [13]. The cut-off limit of T-PSA between prostate hyperplasia and cancer is 4 ng/ml [18]. However, 2.5 ng/ml has recently been recommended as a more accurate cut-off limit [19].

In addition to the geometrical shape and uniformity of the pores, the pore size needs to be adjusted by choosing the appropriate etching conditions, in order to enhance the sensitivity of an interferometer. The pore size has to be large enough to allow biomolecules to enter the pores freely but small enough to retain the optical reflectivity of the pSi surface. If the pore size is not large enough to bind biomolecules with biolinkers in the pores, the sensitivity and reproducibility are deteriorated by the self-aggregation between bio-linkers near the barrier layer.

In this study, the pore size was controlled by pore-widening technique to obtain a higher sensitivity and reproducibility, which could not be obtained with the porous Si [3]. Furthermore, the structure and interference fringe patterns of an AAO chip, fabricated by two-step anodizing process and pore-widening technique depending on the etching conditions employed, were also optimized and characterized in order to lower the detection limit of PSA in an interferometric immunoassay system. The relationships between PSA concentrations and changes in effective optical density (ΔEOT) were investigated according to the pore sizes of the AAO chip function-

†To whom correspondence should be addressed.
E-mail: bwkim@skku.ac.kr

alized with a calyx crown derivative (Prolinker A).

MATERIALS AND METHODS

1. Fabrication of Anodic Aluminum Oxide (AAO) Film

AAO films were fabricated by two-step anodizing process, as reported by Masuda and Fukuda [20] and Hwang et al [21]. Ultrapure aluminum foil with a thickness of 0.5 mm (99.999%, Sigma Aldrich) was cleaned sequentially with acetone, methanol, and distilled water and then was electrochemically polished using the method described in a previous work [4].

The first anodization to obtain alumina (Al_2O_3) film was conducted in a 0.3 M oxalic acid with Pb cathode for 2 h with 40, 50, and 60 V DC at 15 °C. The solution was magnetically stirred to accelerate the dispersion of the heat that evolved from the samples. The second anodization step was also conducted in the same condition as the first step. Meanwhile the oxide layer formed in the first step was removed by wet chemical dissolution in a mixture of phosphoric (6.0 wt%) and chromic (1.8 wt%) acids at 60 °C for an appropriate time depending on the anodization time. Finally, the pores were widened in phosphoric acid solution (5.0 wt%) under a condition dependent on the time according to the target depth and size of the pores.

2. Pt Sputtering and Functionalization of Porous AAO (pAAO) Surface

To increase the surface reflectivity of the oxidized aluminum surface, Pt sputtering was performed at 30 mA/cm^2 and 10^{-2} Torr, to afford a 10 nm-thick Pt layer on the AAO surface. After the AAO surface was washed with EtOH, it was dipped for 24 h in 50 mM of 3-aminopropyltrimethoxysilane, of which the pH was adjusted to 4.5 with acetic acid. After washing and drying for 1 h at room temperature, the surface was purged by N_2 gas to detach any impurities. The silanized surface was functionalized with a 10 mM Prolinker A (Proteogen Co., Seoul, Korea) in $CHCl_3$ solvent for 5 h.

PSA (α2-macroglobulin complex human) and PSA antibody (monoclonal anti-prostate acid phosphatase human from mouse) were purchased from Sigma-Aldrich (St. Louis, MO, USA). To eliminate nonspecific binding, the functionalized AAO surface was stabilized with monoclonal anti-prostate acid phosphatase for 1 h in the incubator, and then washed with PBS (phosphate-buffered silane) buffer.

3. Apparatus and Instrumental Analysis

The interference or fringe pattern was measured in order to quantify the optical characteristics of the pAAO surface. The PSA concentration was determined by measuring wavelength shifts in the Fabry-Perot fringes obtained from pAAO layers, after being exposed to the PSA solution for 30 min and purging with N_2 by using the interferometric biosensing system with a spectrometer (S2000, Ocean Optics, Inc., Dunedin, Florida, U.S.A.), as described in the previous work [5].

AAO substrate morphology (pore size and depth) was analyzed by scanning electronic microscopy (SEM; JSM6700F, FESEM II, JEOL, Tokyo, Japan). Chemical analysis to confirm the functionalized

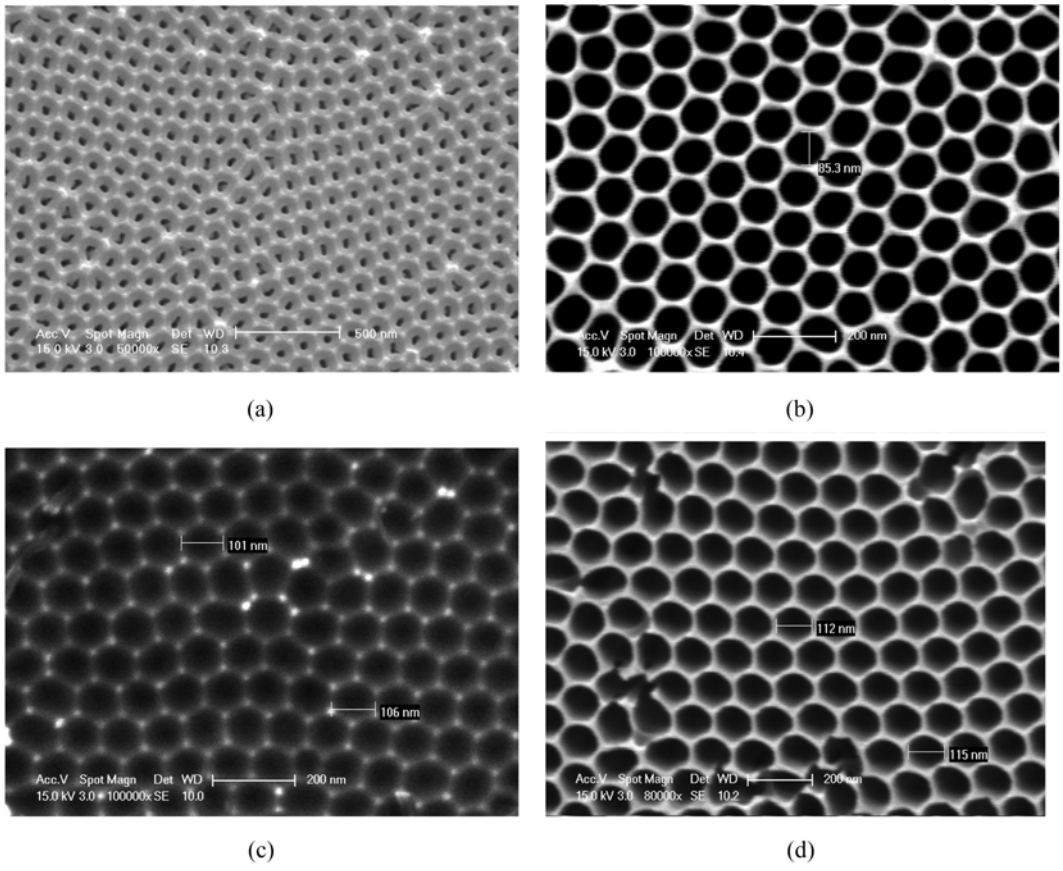

Fig. 1. SEM images of pAAO surfaces at different reaction times of pore widening: (a) before pore widening [4], and at (b) 30 min, (c) 50 min, and (d) 70 min.

layer on the AAO surface was performed with X-ray photoelectron spectroscopy (XPS; ESCA 2000, VG Microtech, East Grinstead, U.K.). The bulk Si sample at each functionalization step was investigated by atomic force microscopy (AFM; CP Research, Thermo Microscopes, California, USA). The reflectivity of the AAO substrates at each fabricating step was analyzed with UV/Vis spectrophotometry (2120UV, Optizen, Daejeon, Korea).

RESULTS AND DISCUSSION

1. Variation of Porous AAO (pAAO) Surface Structure with Pore Widening

The ordering characteristics (ordered pore domains, average pore diameter size and through-pore arrangement) of AAO film are highly affected by the operation conditions (concentration and temperature of electrolyte, voltage and anodizing time) in the two-step anodizing process with oxalic acid electrolyte. Generally, it was reported that the size and density of pores increased with increasing voltage in the anodizing process and that the most uniform pore distribution was obtained at 40 V [7].

In our previous work [4], the pore size range of AAOs obtained by two-step anodizing processes at 40 V as measured by SEM ranged from 30 to 50 nm. Their aspect ratios (pore diameter to depth) ranged from 15 to 20, suitable for application to the interferometer, but their pore sizes needed to be widened to prevent self-aggregation between linkers in narrow pores [4].

In this study, the pores of pAAO fabricated by two-step anodizing were widened in phosphoric acid solution (5.0 wt%). Fig. 1 shows SEM images of pAAO surfaces prepared by the pore-widening method with different reaction times. As the reaction time was increased from 30 to 50 min, the AAO pore size increased approximately up to 80-100 nm, which was about 2-fold larger than the 30-50 nm before pore widening, and some of the pore walls started to crumble away at 70 min.

In a subsequent experiment, pAAO chips with and without pore widening were sputtered with Pt, functionalized with 3-aminopropyltrimethoxysilane and Prolinker A, and then used for PSA detection. The functionalized AAO surfaces were characterized at each reaction step by using XPS, Fourier transform infrared spectrometer (FT/IR), and AFM, as reported by Lee et al. [4].

2. Effect of Pt Sputtering Upon the Porous AAO (pAAO) Surface on the Fringe Pattern Formation

The porous substrates for an interferometer must be transparent to the visible region of the reflectance spectra because a Fabry-Perot fringe pattern is created by multiple reflections of illuminated white light at the top and bottom of the porous substrate layer [3]. As shown in Fig. 2(a), a fringe pattern of the reflectance spectra did not appear in the bare pAAO chip after two-step anodizing, as the chip has a low reflectivity and a uniform distribution of pores that lie very close to each other. Fig. 2(b) shows that the fringe pattern was improved by Pt sputtering that can enhance reflectivity of the pAAO.

To ascertain how reflectivities were changed at each of the pAAO fabrication steps, a UV-VIS spectrophotometer was used to measure the reflectivity (Fig. 3). The reflectivity increased at the annealing step after electropolishing and decreased sharply after the second anodizing step where aluminum is oxidized to alumina (aluminum oxide). After Pt sputtering, the reflectivity recovered to nearly the same level as that before anodizing.

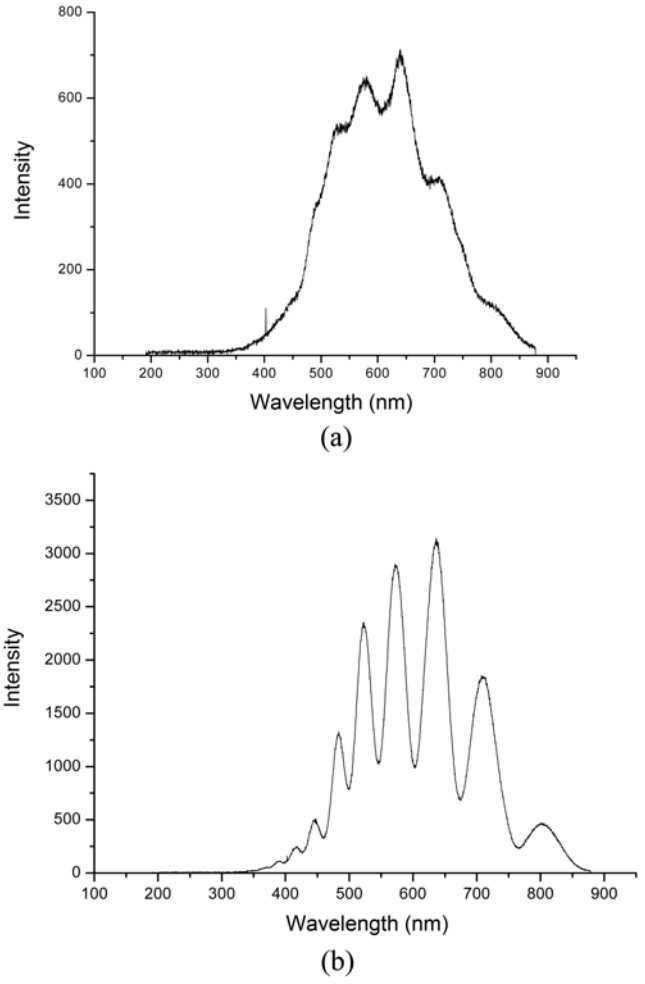

Fig. 2. Interference fringe pattern of a pAAO surface (a) before and (b) after Pt sputtering.

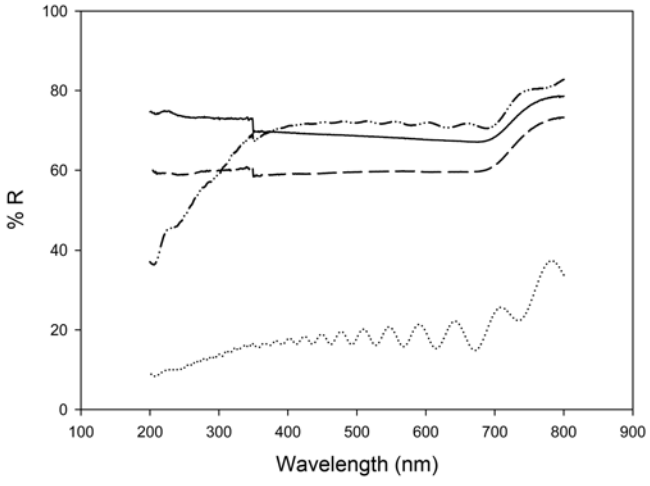

Fig. 3. UV-Vis spectroscopy of an AAO surface at each manufacturing step. Annealing (– –), electropolishing (—), 2nd anodization (·····) and Pt sputtering (–···–).

3. Validation of the Absence of Nonspecific Binding with Bovine Serum Albumin (BSA)

In the protein chip for the immunoassay, the interaction between human fluid proteins and the sensor surface should be minimized [14]. For this purpose, PSA antibody, for combination only with the PSA antigen, was bound with ProLinker A on the surface of

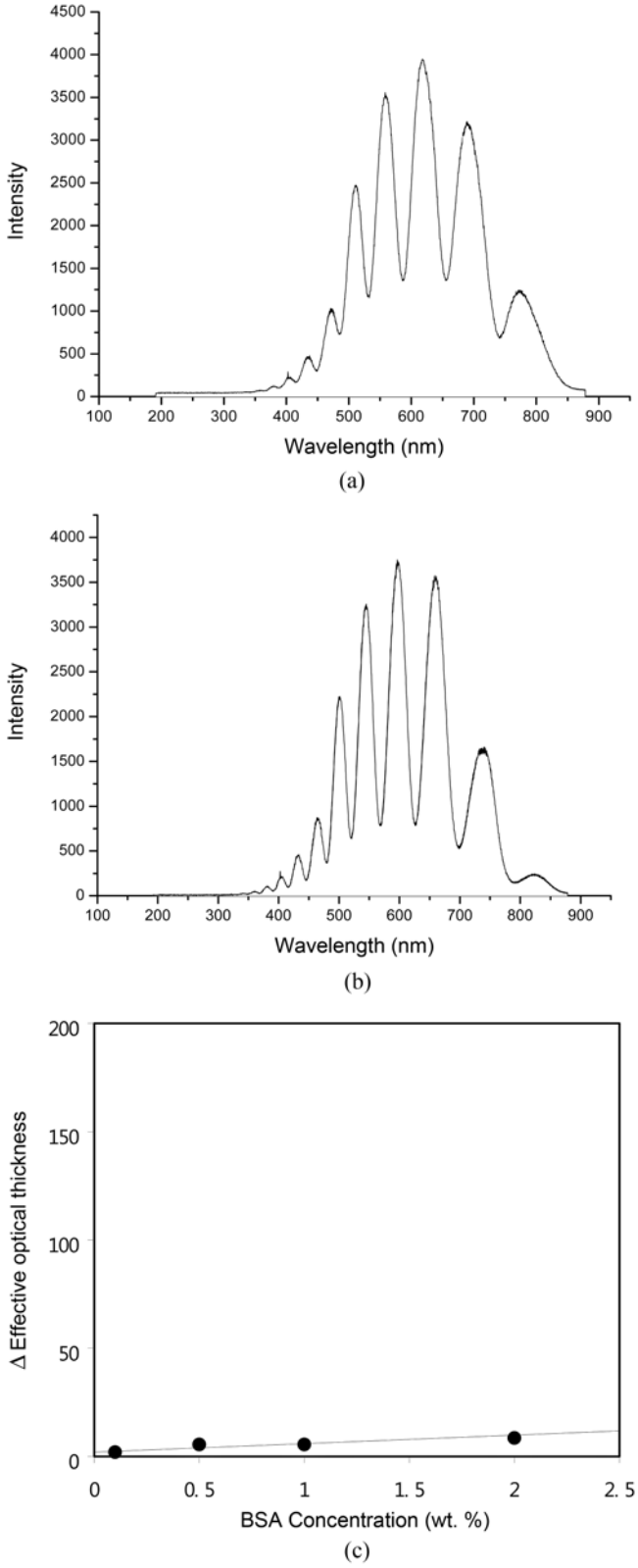

Fig. 4. Interference pattern and difference spectra with BSA: (a) 0.1 wt% BSA, (b) 2.0 wt% BSA, and (c) effect of nonspecific binding of BSA on ΔEOT.

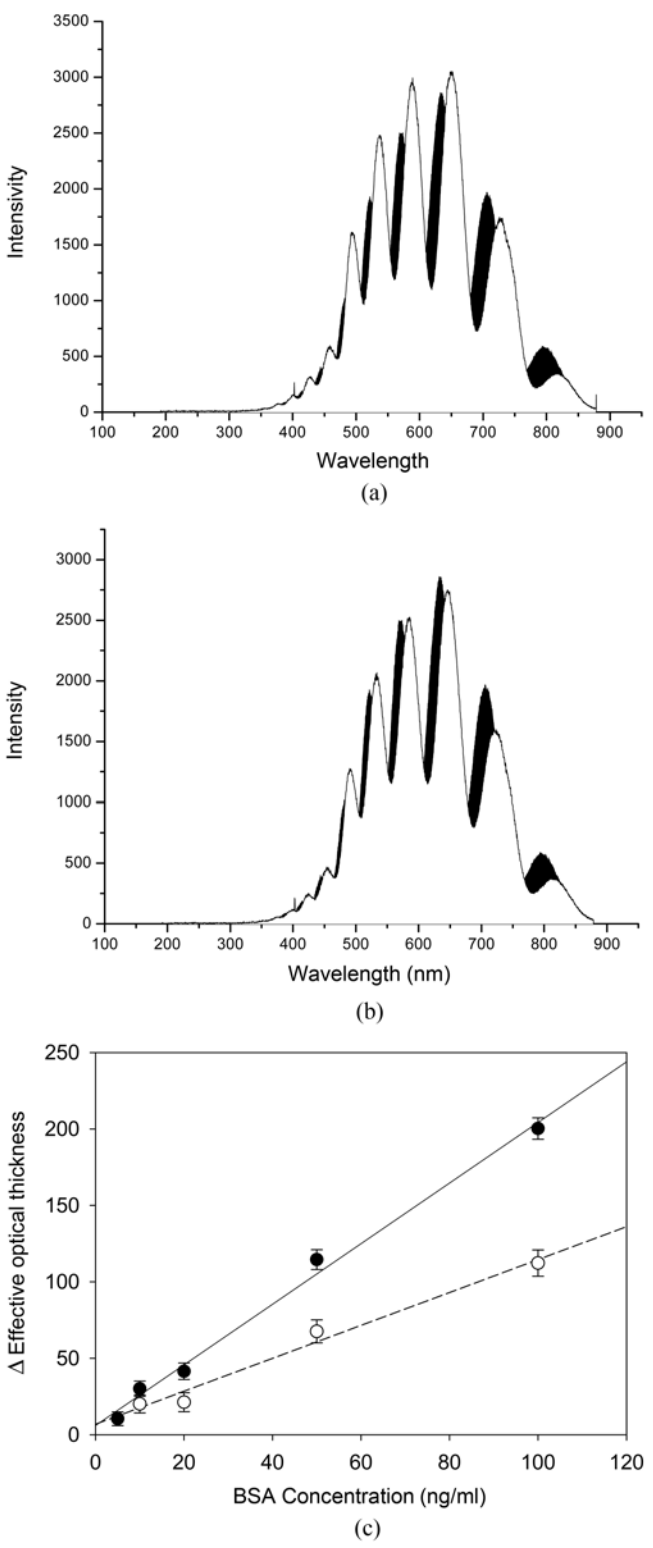

Fig. 5. Interference pattern and difference spectra with 100 ng/ml of PSA: (a) without pore widening and (b) with pore widening (□: deionized water, ■: PSA solution). (c) ΔEOT as a function of PSA concentration (●: with pore widening, ○: without pore widening).

the pAAO chip. To confirm nonspecific binding on the AAO chip, changes in fringe patterns caused by the binding of the common protein present in human serum with the AAO surface materials were investigated by using bovine serum albumin (BSA) at a concentration of 0.1 to 2 wt%. Fig. 4 shows the interference patterns and difference spectra with 0.1 and 2.0 wt% of BSA and the relationship between ΔEOT and BSA concentrations. The shifts in the fringe patterns and ΔEOT affected by the nonspecific binding were nearly negligible, compared with a reference of deionized water, indicating that non-specific binding could be prevented by binding the PSA antibody to a linker on the functionalized pAAO surface.

4. Relationship between PSA Concentration and ΔEOT

To investigate the effect of pore size on the sensitivity, the fringe patterns of the AAO chips with and without pore widening, as well as ΔEOT at the same concentration, were analyzed. As shown in Fig. 5(a-b), the Fabry-Perot fringe pattern of the pAAO chip with pore widening was shifted to a larger wavelength (to the left-hand side) upon exposure to 100 ng/ml of PSA, in comparison with that without pore widening. Fig. 5(c) shows ΔEOT as a function of PSA concentrations (~100 ng/ml). The AAO chip fabricated by pore-widening technique induced a large increase in ΔEOT, indicating that the PSA detection limit can be improved by pore widening. The AAO chip without pore widening did not give a sufficient change in ΔEOT at a PSA level below 20 ng/mL. This result is inadequate for immediate application to an immunoassay for PCa screening. Nevertheless, the results indicate that control over the pore size can positively affect the sensitivity and lower the detection limit.

CONCLUSIONS

We investigated the pore size control of AAO chips in the fabrication steps using the pore widening technique, in order to lower the PSA detection limit. With increasing reaction time for pore widening, the AAO pore size increased approximately two-fold, from 30-50 nm up to about 100 nm, at 50 min, and then some pore walls crumbled away at 70 min. The pAAO chip showed a suitable fringe pattern available for interferometric sensing due to Pt sputtering-enhanced reflectivity. The nonspecific binding exhibited only a negligible effect on ΔEOT, even at a BSA concentration of 0-2 wt%. AAO chips with and without pore widening both showed a linear relationship between ΔEOT and PSA concentration (10-100 ng/ml). However, a large increase in ΔEOT was obtained from the AAO chip with pore widening, confirming that the PSA detection limit can be improved by pore widening.

REFERENCES

1. M. P. Schwartz, S. D. Alvarez and M. J. Sailor, *Anal. Chem.*, **79**, 327 (2007).
2. T. Gao and L. J. Rothberg, *Anal. Chem.*, **79**, 7589 (2007).
3. A. Janshoff, K. P. S. Daucil, C. Steinem, D. P. Greiner, V. S. Y. Lin, C. Gurtner, K. Motesharei, M. J. Sailor and M. R. Ghadiri, *J. Am. Chem. Soc.*, **120**, 12108 (1998).
4. J. C. Lee, J. Y. An and B. W. Kim, *J. Chem. Technol. Biotechnol.*, **82**, 1045 (2007).
5. J. S. Park, S. H. Lim, S. J. Sim, H. Chae, H. C. Yoon, S. S. Yang and B. W. Kim, *J. Microbiol. Biotechnol.*, **16**(12), 1968 (2006).
6. W. Lee, K. Nielsch and U. Gösele, *Nanotechnology*, **18**, 475713 (2007).
7. M. Ghorbani, F. Nasirpouri, A. Irajizad and A. Saedi, *Mater. Des.*, **27**, 983 (2006).
8. G. B. Ji, W. Chen, S. L. Tang, B. X. Gu, Z. Li and Y. W. Du, *Solid State Commun.*, **130**, 541 (2004).
9. I. Lee and R. P. Wool, *Thin Solid Films*, **379**, 94 (2000).
10. R. M. Metzger, V. V. Konovalov, M. Sun, T. Xu, G. Zangari, B. Xu, M. Benakli and W. D. Doyle, *IEEE Trans. Magn.*, **36**, 30 (2000).
11. V. Mizeikisa, S. Juodkazis, A. Marcinkevicius, S. Matsuo and H. Misawa, *J. Photochem. Photobiol. C: Photochem. Rev.*, **2**, 35 (2001).
12. Y. C. Sui and J. M. Saniger, *Mater. Lett.*, **48**, 127 (2001).
13. L. Huang, G. Reekmans, D. Saerens, J. M. Friedt, F. Frederix, L. Francis, S. Muyldermans, A. Campitelli and C. Van Hoof, *Biosens. Bioelectron.*, **21**, 483 (2005).
14. C. Cao, J. P. Kim, B. W. Kim, H. Chae, H. C. Yoon, S. S. Yang and S. J. Sim, *Biosens. Bioelectron.*, **21**, 2106 (2006).
15. S. Wesseling, C. Stephan, A. Semjonow, M. Lein, B. Brux, P. Sinha, S. A. Loering and K. Jung, *Clin. Chem.*, **49**, 887 (2003).
16. C. Fernadez-Sanchez, C. J. McNeil, K. Rawson and O. Nilsson, *Anal. Chem.*, **76**, 5649 (2004).
17. S. P. Balk, Y. J. Ko and G. J. Burbley, *J. Clin. Oncol.*, **21**, 383 (2003).
18. D. A. Healy, C. J. Hayes, P. Leonard, L. McKenna and R. O'Kennedy, *Trends Biotechnol.*, **25**(3), 125 (2007).
19. F. Oberpenning, S. Hetzel, C. Weining, B. Brandt, G. A. Angelis, A. Heinecke, M. Lein, P. Fornara, H. Schmid, L. Hertle and A. Semjonow, *Eur. Urol.*, **43**, 478 (2003).
20. H. Masuda and K. Fukuda, *Science*, **268**, 1466 (1995).
21. S. K. Hwang, S. H. Jeong, H. Y. Hwang, O. J. Lee and K. H. Lee, *Korean J. Chem. Eng.*, **19**, 467 (2002).